

Larmor radius size density holes discovered in the solar wind upstream of Earth's bow shock

G. K. Parks, E. Lee, F. Mozer, and M. Wilber

Space Sciences Laboratory, University of California, Berkeley, California

E. Lucek

Blackett Laboratory, Imperial College, London, United Kingdom

I. Dandouras, H. Rème, and C. Mazelle

Centre d'Etude Spatiale des Rayonnements, Paul Sabatier University, Toulouse, France

J. B. Cao

Key Laboratory for Space Weather, CSSAR, CAS, Beijing, China

K. Meziane

Physics Department, University of New Brunswick, Canada

M. L. Goldstein

NASA Goddard Space Flight Center, Greenbelt, Maryland

P. Escoubet

European Space Agency, Noordwijk, The Netherlands

(Received 20 February 2006; accepted 10 April 2006; published online 22 May 2006)

The Cluster and Double Star satellites recently observed plasma density holes upstream of Earth's collisionless bow shock to apogee distances of ~ 19 and 13 earth radii, respectively. A survey of 147 isolated density holes using 4 s time resolution data shows they have a mean duration of $\sim 17.9 \pm 10.4$ s, but holes as short as 4 s are observed. The average fractional density depletion ($\delta n/n$) inside the holes is $\sim 0.68 \pm 0.14$. The upstream edge of density holes can have enhanced densities that are five or more times the solar wind density. Particle distributions show the steepened edge can behave like a shock. Multispacecraft analyses show the density holes move with the solar wind, can have an ion gyroradius scale, and could be expanding. A small normal electric field points outward. Similarly shaped magnetic holes accompany the density holes indicating strong coupling between fields and particles. The density holes are only observed with upstream particles, suggesting that backstreaming particles interacting with the solar wind are important.

© 2006 American Institute of Physics. [DOI: [10.1063/1.2201056](https://doi.org/10.1063/1.2201056)]

Several transient structures have been reported in the upstream regions of the Earth's bow shock: hot flow anomalies (HFAs),¹ hot diamagnetic cavities (HDCs),² foreshock cavities (FCs)³ and short large-amplitude magnetic structures (SLAMS).⁴ HFAs have durations of a few minutes, scale sizes of about an earth-radius (R_E), strongly fluctuating magnetic fields (\mathbf{B}), and isotropic particles with temperatures (T) that are much greater than that of the solar wind. The bulk plasma flows deviate strongly from those of the solar wind. HFAs are thought to require the interaction of interplanetary current sheets with Earth's bow shock.⁵ Similar properties have been attributed to HDCs, but for these the interior \mathbf{B} and density (n) tend to be the same or slightly lower than those of the surrounding solar wind. In addition, the internal pressure (P) is higher than the ambient solar wind, suggesting HDCs can grow, and account for the edge compressions^{2,6} that can resemble shocks.⁷ In contrast to HFAs and HDCs, FCs have bulk flows that are nearly identical to those in the ambient solar wind, and T and P inside are only slightly greater.³

SLAMS, observed in the quasiparallel shock region, have amplitudes 2–4 times larger than the ambient \mathbf{B} ,⁴ typi-

cal durations of ~ 10 s, and transverse dimensions of an R_E (Refs. 8 and 9) and are thought to grow out of the ultra-low-frequency (ULF) waves. Recently, nonconvective "spiky" electric fields (\mathbf{E}) were measured at the edge of SLAMS.¹⁰ Models of shock with cyclic behavior^{11–13} suggest that Earth's quasiparallel shock is a patchwork of SLAMS slowing down and piling up. SLAMS studies have focused mainly on the magnetic characteristics.

This Letter reports observations of density holes in the upstream solar wind with durations ~ 18 s and depletions ~ 0.7 . We characterize their electromagnetic properties and use four spacecraft observations to show an example of an event with a dimension of an ion gyroradius. We also show that plasma density holes can accompany SLAMS. Data used for this study come from experiments called Cluster Ion Spectrometer,¹⁴ Flux Gate Magnetometer,¹⁵ and Electric Field and Wave.¹⁶

On March 2, 2005, Double Star at 0855 UT (Universal Time) was located at $(11.8, 3.17, 4.96) R_E$ upstream of the bow shock with the four Cluster spacecraft located further upstream at $(12.02, 3.15, 4.8) R_E$ (C1), $(12.09, 2.99, 4.75) R_E$ (C2), $(11.95, 3.13, 4.65) R_E$ (C3), and $(12.18, 3.16, 4.72) R_E$

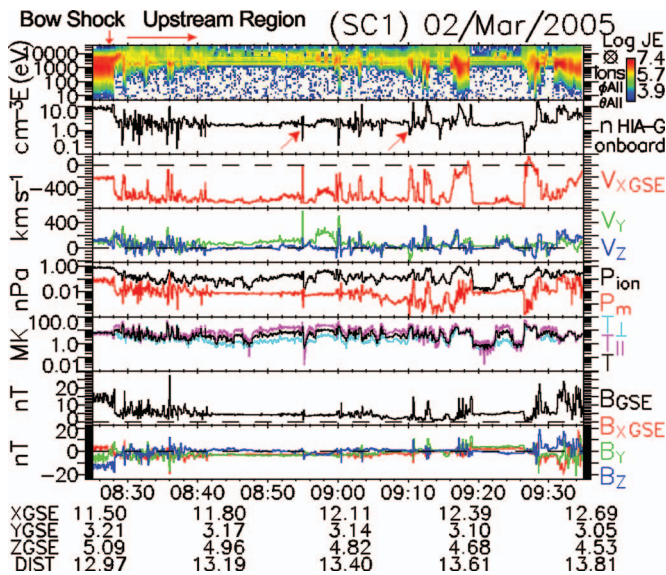


FIG. 1. (Color) Ion and magnetic field measurements obtained by Cluster 1 as it crossed the bow shock into the upstream region. From top to bottom, energy flux, density, bulk velocities in GSE coordinate system, ion and magnetic field pressure followed by the total temperature, and temperatures parallel and perpendicular to \mathbf{B} and total \mathbf{B} and three components. Note that the yellow narrow band above the solar wind H^+ in the top panel is co-moving He^{++} , which shows up at twice the energy per charge in our detector.

(C4) [geocentric solar ecliptic (GSE) coordinates]. Figure 1 shows the transient disturbances detected by the ion and magnetic field experiments as Cluster 1 crossed the bow shock into the upstream region. The magnetosheath in the energy flux spectrogram is a broad energy band while the solar wind is indicated by the narrow red band, at ~ 2 keV. The bow shock crossed C1 at ~ 0829 UT, but moved in and out with shock and magnetosheath plasmas detected several times. The weaker fluxes above the few keV solar wind are the backstreaming particles. The solar wind speed was ~ 600 km/s in the $-V_x$ direction with a density $n \sim 2.5$ cc^{-1} .

Focus now on the sharp dips in n (holes) that go below the average solar wind density (n_{sw}) followed by overshoots above n_{sw} , and which are accompanied by correlated variations in \mathbf{B} (Panels 2, 7, and 8, ~ 0855 and 0901 UT). Examination of data from many crossings indicates that these holes appear in bunches close to the bow shock, but more in isolation at increasing spacecraft distances, all the way to Cluster apogees ($\sim 19 R_E$). The bulk velocities accompanying these dips behave as they do near the bow shock: V_x decreases almost to zero, V_y and V_z deviate substantially, and T increases by an order of magnitude (see Fig. 2 for details).

Figure 2 shows four examples of density holes observed from different bow shock crossings near the subsolar region. These density holes can have symmetric shapes (top left) with n on both edges elevated, or asymmetric with one edge highly elevated (top right). For the events on March 2, 2005, March 3, 2004, and March 1, 2003, shock models indicate quasiperpendicular geometry on the upstream edges and oblique geometry on the downstream edges. The calculated θ_{BN} for downstream (upstream) edges were $\sim 48^\circ$ (57°), 50° ($>75^\circ$), and 45° (72°), respectively. On February 3,

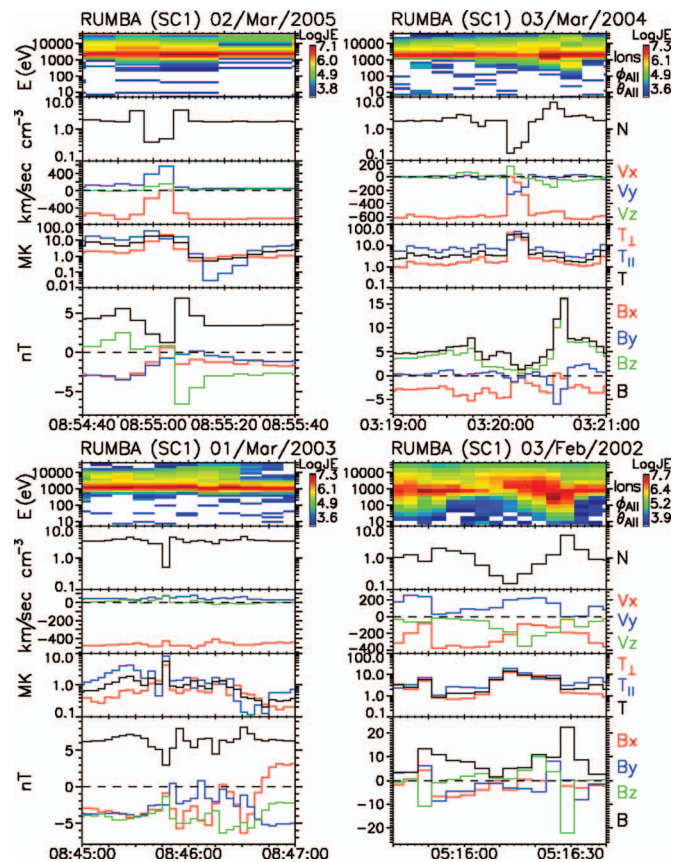


FIG. 2. (Color) Typical examples of ion holes. The density holes are accompanied by nearly identically shaped magnetic holes with reduced intensity in the hole and steepened \mathbf{B} at the edge. The scale of \mathbf{B} is linear, while for n it is logarithmic. Some holes are deep with no measurable particles inside them, while others are shallower with only a factor of 2 decrease in n . The T inside the hole is very hot, more than ten times the solar wind T . The density holes on March 2, 2005 were detected, in GSE coordinates, at $(12.0, 3.2, 4.9) R_E$, on March 3, 2004 at $(9.2, -4.0, 10.5) R_E$, on March 1, 2003 at $(12.6, 3.34, 6.3) R_E$, and on February 3, 2002 at $(9.6, 1.2, -8.5) R_E$.

2002, ULF waves made a θ_{BN} determination problematic, yielding a rough estimate $\sim 30^\circ$ (45°).

A sample of 147 holes observed during six orbits were used for a preliminary characterization. These results shown in Fig. 3 indicate density holes have a mean duration of 17.9 ± 10.4 s and a mean $\delta n/n$ of 0.69 ± 0.15 . The δn represents the difference between the solar wind density and the minimum in the hole. The instrumental time resolution was 4 s and the detection of holes as short as 4 s indicates possible existence of even shorter duration holes. Examination of high resolution spacecraft potential (used as a proxy for n)

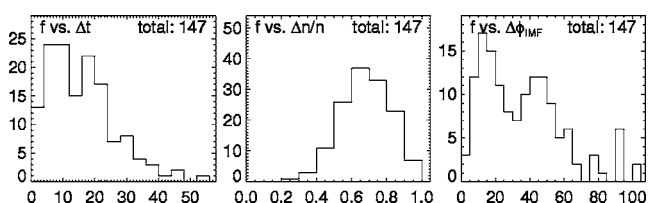


FIG. 3. Number of density holes as a function of duration (Δt), fractional density depletion ($\delta n/n$), and magnetic field rotation from times before to after the hole for 147 density holes observed on five bow shock crossings.

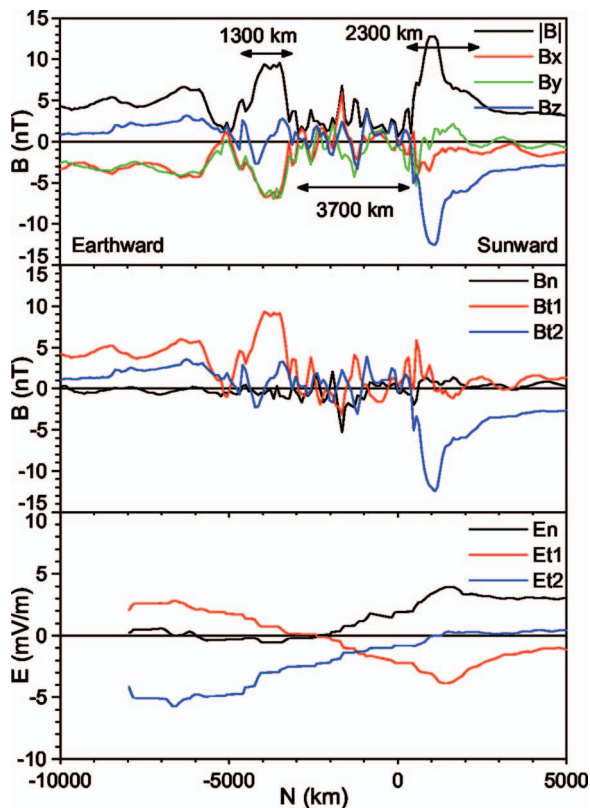


FIG. 4. (Color) Magnetic field profile of the density hole in the Lagrangian format and the behavior of \mathbf{E} and \mathbf{B} in boundary normal coordinates using 22.5 Hz and 25 Hz data, respectively.

at 22.5 times/second and magnetic field (25 Hz) for a few holes showed there were no significant substructures, although fluctuations were present (an example is shown in Fig. 4). The right hand panel of Fig. 3 shows the mean of rotation of the magnetic field across the hole was $\sim 36^\circ \pm 24^\circ$. The density holes are associated with magnetic shears, but the significance of the two peaks is not yet understood.

Ion density holes are accompanied by magnetic holes of nearly the same shape (Fig. 2). The n and \mathbf{B} typically increase by a factor of 2–5 at the edges. The \mathbf{B} -components often rotate from positive (negative) to negative (positive) at the edge, and B_x is small (~ 0) at the minimum of the hole. The density hole observed on February 3, 2002 is associated with a published SLAMS event and the behavior of \mathbf{E} and \mathbf{B} (Refs. 8–10) has been studied in detail, but not that of the ion characteristics.

A density hole detected on March 2, 2005 by both Cluster and Double Star has been analyzed in detail. This hole showed that n at both edges increased from the solar wind value ~ 2 to ~ 3.5 cc^{-1} , while inside the hole, it decreased to ~ 0.45 cc^{-1} . The bulk T rose from $\sim 3 \times 10^5$ to $\sim 2 \times 10^7$ K and V_x decreased from greater than -600 to ~ 0 km/s, while V_y increased from ~ 100 to ~ 600 km s^{-1} . The $|\mathbf{B}|$ variations were in phase with the density, but the \mathbf{B} intensity at the downstream edge increased $\sim 20\%$ (~ 4.5 to ~ 5.5 nT), while at the upstream edge it nearly doubled, ~ 4 to ~ 7 nT. Inside the hole, B decreased to ~ 0.5 nT. The solar

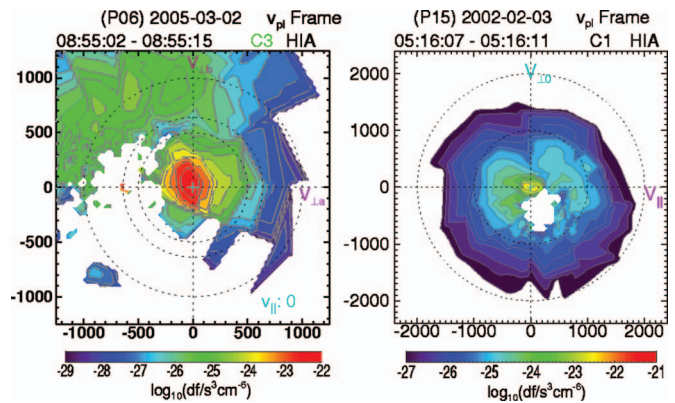


FIG. 5. (Color) Ion phase space distributions of density holes. Left panel: perpendicular \mathbf{B} cut through the main solar wind beam in the upstream edge of the 0855 UT, March 2, 2005 event. Right panel: a distribution obtained within the interior of the 0516 UT, February 3, 2002 density hole.

wind parameters were, $\beta = 8\pi nkT/B^2 \sim 1.6$, $T_e/T_i \sim 2$, $V_A = B/(4\pi nm_i)^{1/2} \sim 56$ km s^{-1} and $c_s = (kT_e/m_i)^{1/2} \sim 90$ km s^{-1} .

A timing analysis from the four Cluster spacecraft assuming a planar geometry yielded a normal $(-0.65, 0.75, 0.065)$ for the downstream edge at 0855 UT and a speed of ~ 530 km s^{-1} along the normal. The normal of the upstream edge was $(-0.80, 0.59, 0.11)$ and the speed ~ 320 km s^{-1} , indicating a significant relative motion. Double Star downstream indicated that the speed of the edges could have changed. The resulting downstream edge acceleration was estimated to be ~ 56 km s^{-2} , and the sunward edge deceleration -23 km s^{-2} . This implies the hole was growing at an increasing rate. (Errors are typically $\sim 10\%$. In the case of acceleration, errors are larger.)

Figure 4 is a Lagrangian plot of this density hole. The size of the downstream edge at Cluster was ~ 1300 km, the upstream edge ~ 2300 km, and the hole ~ 3700 km. (Including acceleration would make them larger.) The gyroradius of 4 keV proton in $B=4$ nT is ~ 1100 km. The growth time of the edges obtained by dividing the width of the hole by the relative velocity of the two edges yields ~ 10 s (including acceleration will reduce this value). The \mathbf{B} at both edges was compressed and the normal component B_n nearly vanished throughout. \mathbf{E} included both tangential E_t , and normal E_n with E_t perpendicular to B_t . Here, $E_t = E_{t1} + E_{t2}$. Measurements of \mathbf{B} inside the hole indicated presence of a small and fluctuating field. (Small fluctuations are also seen in \mathbf{E} but data have been smoothed.)

The left panel of Fig. 5 shows an ion distribution associated with the density hole at ~ 0855 UT, March 2, 2005. This velocity space plot is a cut normal to \mathbf{B} through the main solar wind beam (centered) and shows the nongyrotopic character of the plasma (\mathbf{B} points out of the page.) This three-spin (12 s) integration overlaps the upstream edge of the structure and is time-aliased, but still reveals an arc of ions in the upper left quadrant that appears to be a gyroreflected component similar to those seen at the foot of collisionless shocks. Using the upstream sunward edge normal direction and the speed from timing analysis, we obtained a normal incidence Alfvén Mach number $M_A = 3.3$. The upstream exterior \mathbf{B} was about $(-1, -1, -3)$ nT, which was

$>80^\circ$ from the normal direction, indicating the solar wind flow into this structure was supercritical with a strongly perpendicular geometry. We thus expect that a shock-like boundary might form, and the presence of reflected ions suggests an associated cross-boundary \mathbf{E} field as well (Fig. 4).

A feature not apparent in the left panel of Fig. 5 is revealed in a distribution (right panel) obtained for a density hole observed at ~ 0516 UT on February 3, 2002, (the SLAMS event,¹¹ Fig. 2, lower right). In this case, the slice is through a plane defined by $V_{sw} \times \mathbf{B}$ with \mathbf{B} pointing to the right, and again the main solar wind beam is centered. Comparisons with upstream distributions obtained a few spins later show that the main solar wind beam component is reduced in phase space density by more than an order of magnitude, consistent with the large reduction in overall density n . Also present is a significant suprathermal population that appears much like an upstream intermediate distribution.¹⁵ The temperature in density holes rose to $>10^7$ K, and can be accounted for by the presence of this energetic component and the reduction of the colder solar wind population. While the solar wind beam is observed to slow down and change direction within and at the edges, the measured beam velocity differs from the computed moments, indicating relative motion of the energetic component. The latter ions may originate in backstreaming particles observed exterior to the structure, retaining some of their initial field-aligned momentum.

A necessary condition for the density holes is that backstreaming energetic particles are present although the latter often exists without the former. These periods usually have \mathbf{B} perturbations. Although beam-plasma interactions appear to be important,^{17–19} the details involved in creating the density holes are not known. Examination of the solar wind bulk parameters has thus far not revealed obvious plasma conditions under which density holes are always observed. The density holes occur for solar wind velocities <400 to >800 km/s, $n \sim 1–10$ /cc, and $T \sim 10^5–10^6$ K. Deep density holes with large edge enhancements can have shallow magnetic holes and weak \mathbf{B} overshoots, while shallow density holes with weak edge enhancements can have deep magnetic holes and large overshoots.

Density holes have significant bulk flow deflections, are filled with heated plasma, have enhanced edge densities, and one or both edges have compressed magnetic field and tens of keV energetic electrons.⁶ The density holes have durations similar to those of SLAMS but which are much shorter than HFAs and HDCs, and correspondingly smaller dimensions. The order of magnitude density depletions have not been reported previously for HFAs, HDCs, or SLAMS. Density holes appear to be fairly common while HFAs and HDCs occur rarely. Only eight HFA events have been reported in ISEE observations spanning more than two years,² and the

combined number including HDCs observed by ISEE, AMPTE-IRM, and AMPTE-UKS was about 30.⁵

All of the published SLAMS events seen by Cluster have density holes associated on the downstream edge (not shown). We have shown one example of a SLAMS event that has a density hole with already “heated” backstreaming plasmas associated with it. In addition, the density holes near the shock tend to have elevated edges that account for more particles than those depleted within the hole. The heating plus the net gain in particles is consistent with what is observed across the shock transition, and reflects as expected net density increases within structures moving relative to the solar wind flow.

We have presented first observations of ion gyroradius-scale density hole structures in the upstream solar wind. Future work will include examination of high frequency electromagnetic and electrostatic wave data and a more detailed study of electron observations, in order to establish the roles of wave particle interactions. Improved statistics on upstream plasma and beam parameters (density, speed, T , Mach number, plasma β , and shock geometry) may reveal factors controlling their origin and development.

The research at UC Berkeley was performed under a NASA Grant No. NNG04GF23G. Cluster is a joint project of ESA and NASA, and Double Star is a joint project of the ESA and the Chinese Space Agency. We acknowledge the International Space Science Institute in Bern, Switzerland for their support of the “Production and Transport of 1–30 keV Upstream Ions” science team.

¹S. J. Schwartz, C. P. Chaloner, P. S. Christiansen *et al.*, *Nature* (London) **318**, 269 (1985).

²M. F. Thomsen, J. T. Gosling, S. A. Fuselier *et al.*, *J. Geophys. Res.* **91**, 2961 (1986).

³D. G. Sibeck, T.-D. Phan, and R. Lin, *J. Geophys. Res.* **107**, 1271 (2002).

⁴S. J. Schwartz *et al.*, *J. Geophys. Res.* **97**, 4209 (1992).

⁵S. J. Schwartz *et al.*, *J. Geophys. Res.* **105**, 12639 (2000).

⁶G. Paschmann, G. Haerendel, N. Sckopke *et al.*, *J. Geophys. Res.* **93**, 11279 (1988).

⁷S. A. Fuselier, M. F. Thomsen, J. T. Gosling *et al.*, *J. Geophys. Res.* **92**, 3187 (1987).

⁸E. A. Lucek, T. S. Horbury, M. W. Dunlop *et al.*, *Ann. Geophys.* **20**, 1699 (2002).

⁹E. A. Lucek, T. S. Horbury, T. S. Balogh *et al.*, *Ann. Geophys.* **22**, 2309 (2004).

¹⁰E. Lucek, T. S. Horbury, A. Balogh *et al.*, *J. Geophys. Res.* **109**, A06207 (2004).

¹¹R. Behlke *et al.*, *Geophys. Res. Lett.* **30**, 1177 (2003).

¹²D. Burgess, *Geophys. Res. Lett.* **16**, 345 (1989).

¹³S. J. Schwartz and D. Burgess, *Geophys. Res. Lett.* **18**, 373 (1991).

¹⁴H. Réme *et al.*, *Space Sci. Rev.* **79**, 303 (1997).

¹⁵A. Balogh *et al.*, *Space Sci. Rev.* **79**, 65 (1997).

¹⁶G. Gustafsson, R. Boström, B. Holback *et al.*, *Space Sci. Rev.* **79**, 137 (1997).

¹⁷M. Scholer, *J. Geophys. Res.* **98**, 47 (1993).

¹⁸Y. Lin, *J. Geophys. Res.* **102**, 24265 (1997).

¹⁹V. A. Thomas and S. H. Brecht, *J. Geophys. Res.* **93**, 11341 (1988).